MODELING OF HYDROGEN PRESSURIZATION AND EXTRACTION IN CRYOGENIC PRESSURE VESSELS DUE TO VACUUM INSULATION FAILURE

Moreno-Blanco, J.C.[1], Elizalde-Blancas, F.[1], Gallegos-Muñoz, A.[1], and Aceves, S.M.[2]
[1] Mechanical Engineering Department, University of Guanajuato, Carretera Salamanca - Valle de Santiago Km. 3.5 + 1.8, Salamanca, Guanajuato, 36885, Mexico, jc.morenoblanco@ugto.mx
[2] Lawrence Livermore National Laboratory, 7000 East Avenue, Livermore, CA, 94550, USA, aceves6@llnl.gov

ABSTRACT

We have analyzed vacuum insulation failure in an automotive cryogenic pressure vessel (also known as cryo-compressed vessel) storing hydrogen (H_2). Vacuum insulation failure increases heat transfer into cryogenic vessels by about a factor of 100, potentially leading to rapid pressurization and venting to avoid exceeding maximum allowable working pressure (MAWP). H_2 release to the environment may be dangerous if the vehicle is located in a closed space (e.g. a garage or tunnel) at the moment of insulation failure. We therefore consider utilization of the hydrogen in the vehicle fuel cell and electricity dissipation through operation of vehicle accessories or battery charging as an alternative to releasing hydrogen to the environment. We consider two strategies: initiating hydrogen extraction immediately after vacuum insulation failure, or waiting until MAWP is reached before extraction. The results indicate that cryogenic pressure vessels have thermodynamic advantages that enable slowing down hydrogen release to moderate levels that can be consumed in the fuel cell and dissipated onboard the vehicle, even in the worst case when the vacuum fails with a vessel storing hydrogen at maximum refuel density (70 g/L at 300 bar). The two proposed strategies are therefore feasible and the best alternative can be chosen based on economic and/or implementation constraints.

1. INTRODUCTION

Hydrogen (H_2) is a strong candidate to replace hydrocarbons as transportation fuel, with the advantage of eliminating environmental pollution during both production and utilization. Its physical and chemical properties make it superior to fossil fuels, because it is the simplest, lightest molecule and has the capability of generating clean and efficient energy while producing only water and no CO_2. However, its main disadvantage is its low energy density compared to hydrocarbons, thus its widespread use has been limited [1].

The concept of using hydrogen as a substitute for hydrocarbons is not new. However, in comparison to hydrocarbons, H_2 storage and delivery are challenging. The simplicity of the H_2 molecule results in low density, occupying in liquid state (saturated at 20.2 K and 1 bar) about four times more volume per unit of energy than gasoline [1]. The storage method will be determined by the final application, and must be cost competitive [2]. The two most viable options from technical (in which safety plays a key role) and economical points of view are hydrogen storage as liquid and as compressed gas [3, 4].

Liquid hydrogen (LH_2) is most widely used for large-scale storage. In vehicles, however, compressed gas currently dominates even though it requires expensive high-pressure vessels. LH_2 is denser (up to 70 kgH_2/m^3 vs. ~40 kgH_2/m^3 for compressed gas), potentially leading to lower distribution and onboard storage cost in automobiles [1]. However, hydrogen losses during periods of inactivity have limited its use. LH_2 vessels are typically built for low pressures, with ~5 bar maximum allowable working pressure (MAWP). In pressure vessels, MAWP is the relief device setting, where H_2 is released to avoid overpressurization. At 5 bar MAWP, short periods of inactivity (2-3 days) pressurize the vessel enough to demand H_2 release, even for very well insulated vessels (1-3 W/m^2).

An alternative has recently arisen: the possibility of storing hydrogen in cryogenic vessels that can operate at high pressure [5-9]. Also known as cryo-compressed vessels, these cryogenic pressure vessels consist of a high-pressure (300-350 bar MAWP) metal lined, fiber-wrapped (type 3) inner vessel, a vacuum space containing numerous sheets of highly reflective metalized plastic (multilayer insulation,

MLI), and an outer metallic jacket. Cryogenic pressure vessels enable substantial reduction or elimination of H_2 losses resulting from hydrogen pressurization beyond MAWP as a consequence of heat transfer from the environment, because (1) heat transfer from the environment is reduced to very low values (1-3 W/m^2) due to vacuum insulation, (2) the vessel is filled with liquid or cryogenic pressurized gaseous hydrogen, both of which have very low entropy, minimizing heating during the fill process, and (3) hydrogen is typically extracted from the vessel at higher temperature and entropy, thus extraction results in considerable cooling and depressurization of the hydrogen stored in the vessel. The proposed vessels have successfully completed a series of certification tests through three generations of prototypes [5-7]. Research to date shows that cryogenic pressure vessels enable higher storage capacity, increasing vehicle autonomy. They are also lighter and have the lowest ownership cost of all available hydrogen storage technologies [10].

Cryogenic pressure vessels also present compelling safety advantages. Several studies have analyzed the sudden expansion and release of hydrogen subsequent to vessel failure [11-13], and it has been demonstrated that released energy is significantly reduced due to operation at cryogenic temperature, even if storage pressure is high. The vacuum jacket reduces venting pressure by one order of magnitude, and other parameters such as energy release rate and thrust are considerably lower than in compressed gas vessels [12, 14-17].

In this paper, we consider a previously unexplored safety aspect of cryogenic pressure vessels: the failure or leakage of the outer metallic jacket with the consequent loss of vacuum and sudden increase (~100X) in heat transfer from the environment. Under these conditions, it is possible that a fraction of hydrogen may need to be released to the environment in order to avoid exceeding the MAWP. Release of hydrogen could result in a dangerous situation if it occurs when the vehicle is parked in an enclosed space (e.g., a garage or tunnel) [18].

A safer alternative to releasing hydrogen to the environment is *consuming* the extracted hydrogen. Depending on the extraction rate, it could be possible to consume the hydrogen in the vehicle fuel cell and dissipate the electricity generated by e.g. operating the vehicle accessories (mainly the air conditioner) or recharging the battery. It is therefore critical to calculate the rate at which hydrogen needs to be extracted from the cryogenic pressure vessel and the electric power generated to determine if it is possible to (1) consume the hydrogen in the fuel cell, and (2) dissipate the electricity generated by the fuel cell onboard the vehicle.

We calculate the hydrogen extraction rate according to two different strategies: (1) Initiate hydrogen extraction immediately upon vacuum vessel failure. This strategy minimizes hydrogen extraction rate, but demands vacuum sensors or continuous monitoring of pressurization rate to determine vacuum failure. (2) Wait until the vessel reaches MAWP before starting hydrogen extraction. Although this second strategy requires faster hydrogen extraction, it does not require sensors or calculations and thus it could be the preferred option if the amount of extracted hydrogen can be consumed and the generated electric power can be dissipated onboard the vehicle.

2. ANALYSIS

The cryogenic pressurized hydrogen storage system includes a high-pressure inner vessel, a vacuum space filled with many layers of reflective plastic (multilayer insulation, MLI) that serves as thermal insulator, and an outer metallic jacket. We consider an inner vessel manufactured by Worthington Industries. This is a commercially available Type 3 (aluminum lined, fiber wrapped) vessel. Its main characteristics are listed in Table 1. We assume the worst case in which the cryogenic vessel stores hydrogen at high density and pressure (70 kg/m^3, 300 bar, 57.8 K) when the loss of vacuum occurs. At this condition, typical of maximum filling capacity [19], the vessel stores 7.91 kg of gaseous cryogenic H_2 in the internal volume of 113 L. We assume 300 K ambient temperature.

Table 1. Specifications of the high-pressure inner vessel (ALT-890, Worthington Industries).

Outer diameter	333 mm
Length	1778 mm
Internal volume	113.1 L
Weight	82.2 kg
Maximum operation pressure (MOP)	350 bar
Maximum allowable working pressure (MAWP)	437 bar
Weight fraction of aluminum and composite	50% Al, 50% comp.
Vacuum insulation thickness	2 cm

2.1 Heat transfer, pressurization and hydrogen release model

The inner vessel is characterized with a lumped model that assumes uniform and equal temperature of H_2 and vessel. This is justified because of (1) the high thermal conductivity of H_2 and aluminum, and (2) the slow heating process (hours) that allows thermal equilibration between H_2 and the wall.

We start analyzing the vessel as a closed system. This is applicable to the initial process of vessel heating from a pressure lower than the MAWP when there is no need to extract hydrogen. We later analyze heating with hydrogen extraction at constant pressure (equal to MAWP).

The energy equation for the inner vessel is:

$$\frac{dU_T}{dt} = \dot{Q}_i - \frac{dU_g}{dt}, \tag{1}$$

where U_T and U_g are the internal energy of the vessel and hydrogen, respectively. For the open system, the vessel mass conservation equation is,

$$\frac{dm_{VC}}{dt} = -\dot{m}_{H_2} \quad \rightarrow \quad dm_{VC} = -\dot{m}_{H_2} \cdot dt, \tag{2}$$

whereas the energy conservation equation for the inner high pressure vessel is,

$$\frac{dU_T}{dt} = \dot{Q}_i - \frac{dU_g}{dt} - \dot{m}_{H_2} \cdot h_s, \tag{3}$$

where $\dot{m}_{H_2}$ and h_s are mass flow rate and specific enthalpy of hydrogen released from the vessel.

Considering that the inner pressure vessel is made of an aluminum liner and a carbon fiber overwrap, its internal energy is the sum of the internal energy of each material. Thus, for Eqs. 1-3, the internal energy of the pressure vessel is,

$$U_T = \left(X_{Al} \cdot u_{Al} + X_C \cdot u_C \right) \cdot M_T, \tag{4}$$

where, X_{Al} and X_C are the aluminum and composite mass fractions, u_{Al} and u_C are the specific internal energy of aluminum and composite, and M_T is the total mass of the inner vessel.

When the vacuum vessel fails, air enters the MLI-filled vacuum space. The vessel is wrapped in many layers of shiny plastic in an arrangement geometrically similar to narrowly spaced concentric cylinders. We can therefore model heat transfer into the vessel by considering the competition between air conduction and natural convection between concentric cylinders according to a published procedure

[20]. The results indicate that conduction heat transfer dominates the process. Natural convection is negligible because the narrow spacing between MLI sheets (typically 1 mm) restricts air flow. Radiation heat transfer is also negligible compared with conduction through air due to the many layers of reflective plastic. Hence, heat transfer to the inner vessel is,

$$\dot{Q}_i = A_T k_{air} \frac{\left(T_\infty - T_{H_2}\right)}{L_T}, \tag{5}$$

where, A_T is the external surface area of the internal vessel, k_{air} is the air thermal conductivity, T_∞ is the temperature of the outer metallic jacket, T_{H_2} is the hydrogen temperature contained in the vessel and L_T is the thickness of the vacuum space. The thermal conductivity of air at 300 K is 26.3×10^{-3} *W/m-K* decreasing to 8×10^{-3} *W/m-K* at 90 K. We conservatively use the air thermal conductivity at 300 K because it maximizes heat transfer and pressurization rate.

2.2 Thermophysical properties of hydrogen

It is assumed that the vessel is initially filled with para-hydrogen, the dominant phase at cryogenic temperature, which is characterized by an antiparallel nuclear spin. Hydrogen at the conditions of interest for this problem does not behave as an ideal gas. Leachman [21] has developed formulations to calculate the thermodynamic properties of para-hydrogen. Leachman's model, programmed in the software REFPROP version 8.0 [22], has been widely used in the literature for the calculation of H_2 properties at low temperatures and high pressures; we therefore use REFPROP for the prediction of para-H_2 properties through the link with Matlab® for the solution of the mathematical model.

2.3 PEM fuel cell model

Hydrogen consumption in the PEM fuel cell can be modeled as follows [23, 24]: The fuel cell efficiency is defined as,

$$\eta_{fc} = \frac{Electrical\ \ power\ output}{Heating\ \ power\ of\ \ inlet\ Fuel} = \frac{P_{fc}}{F_{in}}, \tag{6}$$

where the electric power output is $P_{fc} = V_{fc} \cdot I_{fc}$, and the heating power of the inlet fuel is,

$$F_{in} = \frac{M_{H_2} \cdot \Delta HHV}{nF} \cdot I_{fc} \quad \rightarrow \quad \Delta HHV = 142000\ J/g$$
$$F_{in} = 1.482 \cdot I_{fc} \tag{7}$$

where the hydrogen higher heating value (ΔHHV) is taken as the reference. Thus,

$$\eta_{fc} = \frac{V_{fc}}{1.482}, \text{ and}$$

$$I_{fc} = \frac{P_{fc}}{1.482 \cdot \eta_{fc}} \tag{9}$$

Therefore, the hydrogen mass flow rate extracted from the vessel and supplied to the fuel cell is,

$$\dot{m}_{H_2} = \frac{P_{fc} \cdot M_{H_2}}{1.482 \cdot n \cdot F \cdot \eta_{fc}}, \quad (11)$$

where F is Faraday constant (96485 Coulomb/mol), M_{H_2} is the molecular weight of H_2 (0.002016 kg/mol), and n is the number of electrons per H_2 molecule (2) involved in the reaction. We assume 36% fuel cell efficiency based on H_2 HHV [25] as a typical value for automotive propulsion.

3. RESULTS

3.1 Pressurization without hydrogen release

Fig. 1(a) shows hydrogen pressure as a function of time for several densities, assuming that hydrogen is heated from 20 K in a constant density process (without hydrogen release). The dotted line in Fig. 1(a) corresponds to the vessel maximum allowable working pressure (MAWP, 437 bar). It can be noted that the vessel filled to 70 g/L pressurizes to 437 bar in only 2 hours, whereas the vessel filled to 40 g/L takes considerably longer (about 14 hours) to reach MAWP. Other densities in Fig. 1(a) are too low for the vessel to reach MAWP.

From the temperature vs. time results (Fig. 1b) we observe rapid initial warming followed by slower temperature rise after the first few hours. This is because heat transfer (Fig. 1c) is proportional to the temperature difference between the vessel and the environment, which drops as the vessel is heated. In addition to this, specific heats of both vessel and hydrogen increase with temperature. The vessels containing more hydrogen have a higher heat capacity that allows them to stay cold for longer time, even though they are exposed to faster heat transfer.

Fig. 2 shows vessel pressure as a function of H_2 density when the vessel reaches thermal equilibrium with the environment (300 K). The figure shows that the maximum hydrogen density that will not exceed the MAWP is 27.4 kg/m^3 (3.1 kg vessel capacity); thus, if the vehicle is parked when the vessel has lower density, there is no need to release hydrogen. Even if vacuum insulation is lost, no safety action is necessary.

On the other hand, it is also concluded that hydrogen extraction is necessary whenever the density at the moment of vacuum insulation failure is greater than 27.4 kg/m^3. Considering a vehicle that is parked when the vessel is full at 300 bar and 70 kg/m^3, it would be necessary to release 4.81 kg of hydrogen to complete the process and ensure that the MAWP will not be exceeded. The key for safe hydrogen extraction subsequent to vacuum loss is maintaining a slow hydrogen extraction rate that can be (1) consumed in the fuel cell to generate electricity, and (2) converted to electricity at a low enough power that can be dissipated onboard the vehicle.

In the following sections the hydrogen extraction rate is calculated for a vessel initially full at 300 bar and 70 kg/m^3. As previously discussed, we first consider Strategy 1 in which hydrogen extraction begins at the time of failure of the vacuum system. We then consider the possibility of delaying hydrogen extraction until vessel MAWP is reached (Strategy 2).

3.2 Strategy 1. Heating with immediate hydrogen extraction

Fig. 3 shows hydrogen pressure as a function of time during the extraction process for several fuel cell output powers assuming that hydrogen extraction starts at the moment of vacuum insulation failure. It is observed that increasing the output power reduces the maximum pressure. The minimum output power at which the fuel cell must be operated to avoid exceeding the MAWP is 6.5 kW, which for 36% fuel cell efficiency corresponds to 1.26x10^{-4} kg/s (0.454 kg/h) hydrogen extraction rate.

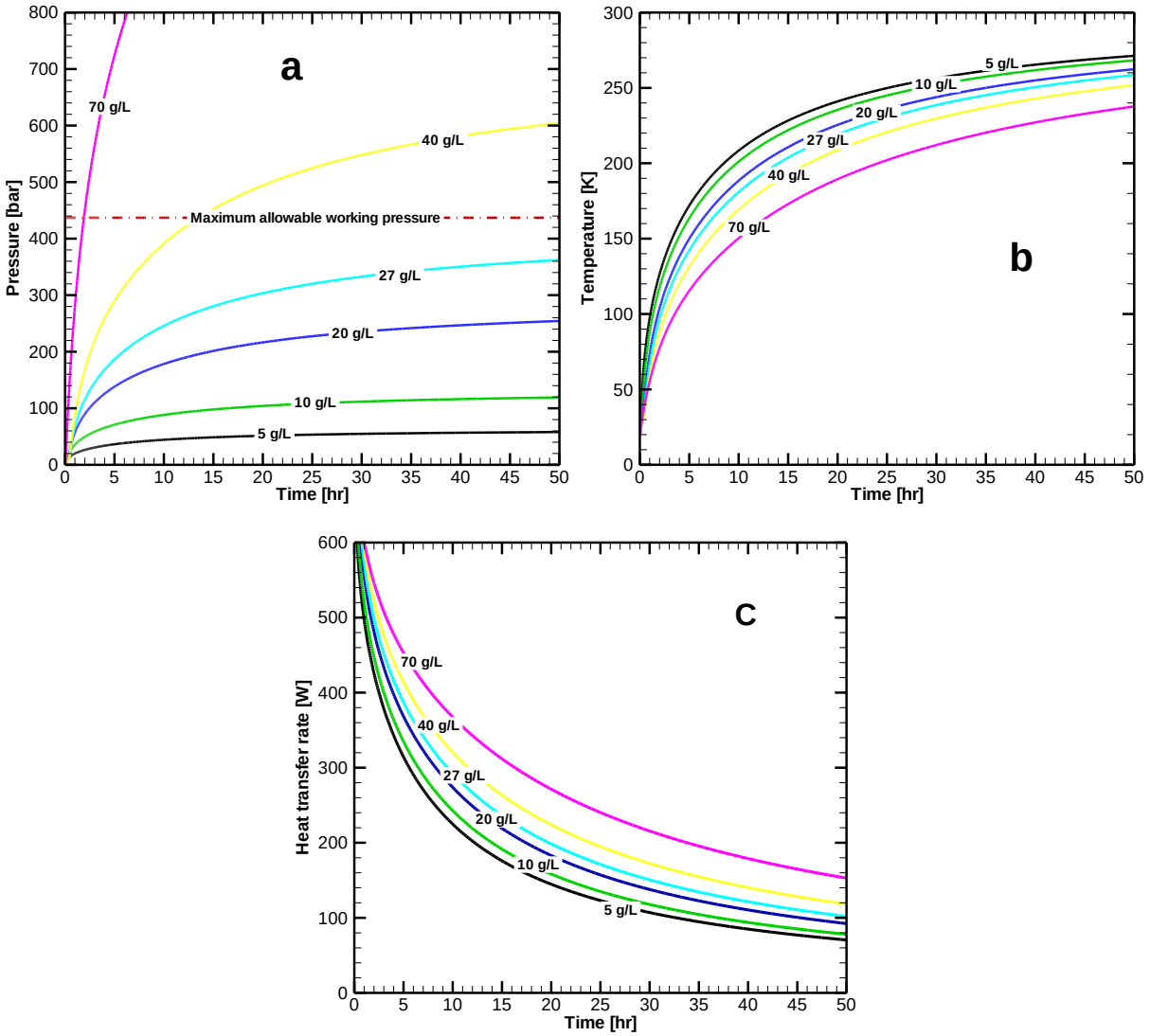

Figure 1. a) Pressure, b) temperature, and c) heat transfer as a function of time for several densities during the heating process subsequent to vacuum loss, assuming heating at constant density without hydrogen extraction.

Fig. 4 shows pressure, density, temperature, and mass flow rate of extracted hydrogen as a function of time, considering a vessel initially at 300 bar and 70 kg/m^3 and the minimum hydrogen extraction rate (1.26×10^{-4} kg/s) sufficient to maintain the pressure at or below MAWP. From Fig. 4 it can be noticed that the MAWP (437 bar) is reached 2.7 hours after hydrogen extraction has started. Once the MAWP is reached, it is possible to keep the vessel at constant pressure (MAWP) while continuously reducing the flow of extracted hydrogen and the output power of the fuel cell, therefore facilitating the task of dissipating the generated electricity.

3.3 Strategy 2. Heating with extraction at maximum allowable working pressure

Waiting until the vessel reaches MAWP before extracting H_2 increases the necessary extraction rate and therefore the electricity produced by the fuel cell and dissipated onboard the vehicle.

Fig. 5 shows pressure as a function of time for several values of fuel cell power for the case of H_2 extraction at MAWP. As shown in Fig. 5, it takes only 40 minutes to pressurize the vessel at constant density (without H_2 extraction) from 300 to 437 bar (MAWP). Considering that H_2 extraction starts at MAWP, it is necessary to extract H_2 at a fast-enough rate to prevent any further pressurization. From Fig. 5, it can be observed that 10.8 kW of fuel cell output power (2.10×10^{-4} kg/s, 0.756 kg/h extraction

rate), is the minimum necessary to avoid exceeding the MAWP. This output power is 66% higher than previously calculated for H_2 extraction at the moment of vacuum insulation failure.

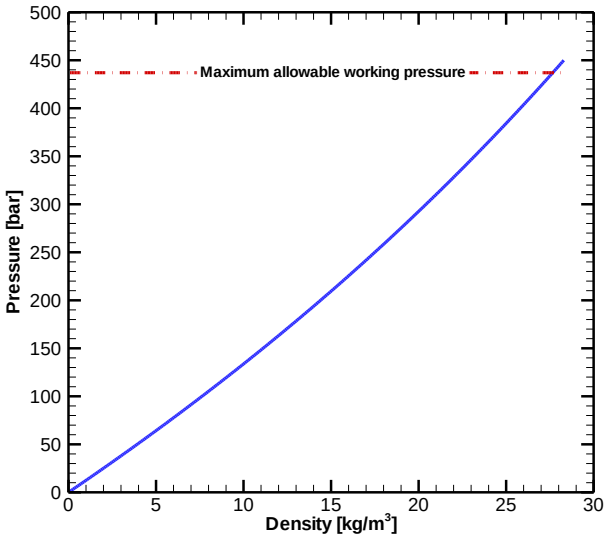

Figure 2. Hydrogen pressure as a function of density when the vessel reaches thermal equilibrium with the environment at 300 K.

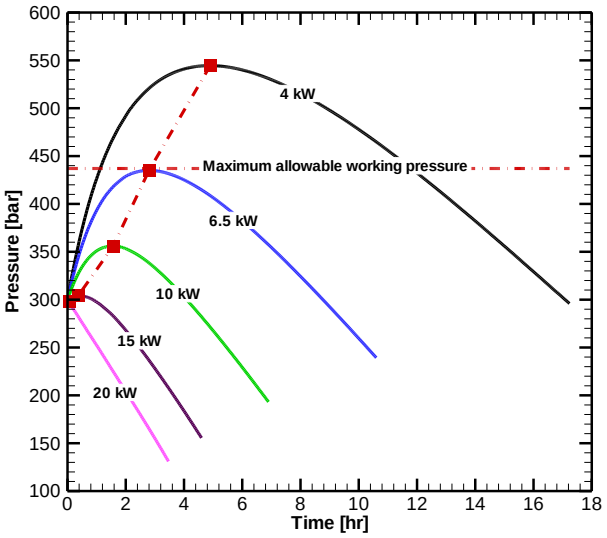

Figure 3. Hydrogen pressure for several fuel cell powers, for a vessel initially filled to 300 bar and 70 kg/m^3, considering that H_2 extraction begins at the moment of vacuum insulation failure (Strategy 1).

Once H_2 extraction starts, the flow rate necessary to maintain the pressure constant at MAWP slows down rapidly (Fig. 6) because H_2 warms up as the extraction process proceeds (see temperature line in Fig. 6), and isentropic extraction is more effective for vessel depressurization as temperature increases.

Fig. 7 includes the information of Figs. 4 and 6 in a single chart to facilitate a detailed comparison between the two strategies. The solid lines represent Strategy 1 (immediate extraction) and the dotted lines correspond to Strategy 2 (extraction at MAWP). Fig. 7 shows that, despite the large initial difference in extraction mass flow rate, the solutions converge once both pressure curves reach MAWP. From then on (2 hours and 40 minutes after vacuum failure), the solid lines and the dotted lines show similar results.

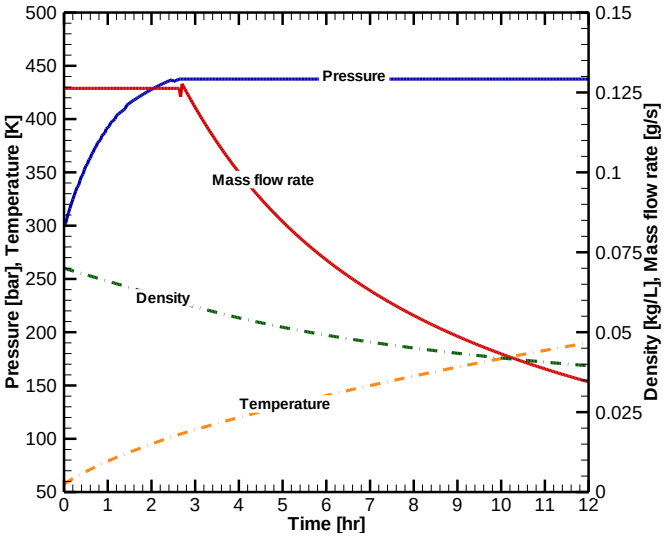

Figure 4. Pressure, mass flow rate, density and temperature of H_2 as a function of time for the heating process with immediate H_2 extraction (Strategy 1) for a vessel initially filled at 300 bar and 70 kg/m^3 (57.7 K) and H_2 extraction at the minimum initial rate (1.26x10^{-4} kg/s, 6.5 kW fuel cell power) to avoid exceeding MAWP.

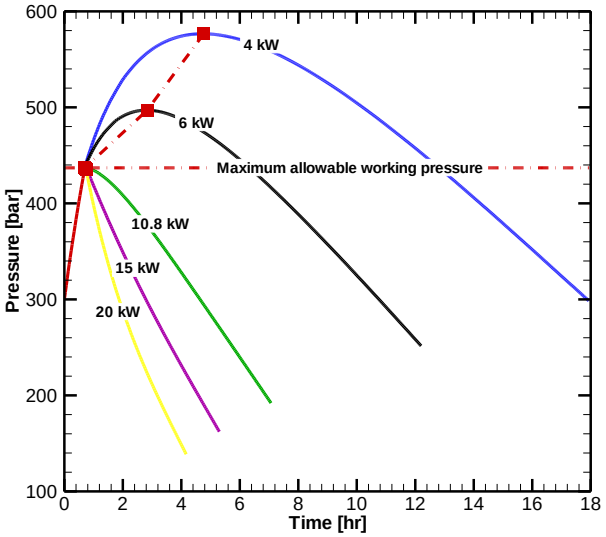

Figure 5. Hydrogen pressure for several fuel cell powers, for a vessel initially filled to 300 bar and 70 kg/m^3, considering that H_2 extraction begins at the moment of reaching MAWP (Strategy 2).

The electricity generated by the fuel cell after vacuum failure has to be properly dissipated. Considering that we assume vacuum failure of a parked vehicle, it may be most appropriate to dissipate the electricity in vehicle accessories. It is therefore important to compare the maximum power with both strategies (6.5 kW and 10.8 kW) with the power that can be consumed by the accessories of a typical vehicle, especially the air conditioner which consumes the most energy. A literature review reveals that depending on compressor speed, air conditioning can consume 1-4 kW [26], almost enough to consume all the produced electricity in Strategy 1. Surplus electricity could then be used for charging the battery. Strategy 2, however, could require incorporating electric resistances to consume all the electricity. These resistances are inexpensive and their input power would drop rapidly as the vessel is emptied (Fig. 6), reducing the risk of overheating sensitive components. In conclusion, both strategies seem to be feasible. One strategy requires identifying the failure of the vacuum system and the other may require the use of additional electric resistances to consume the electricity. The final decision will depend on the economic balance between both strategies.

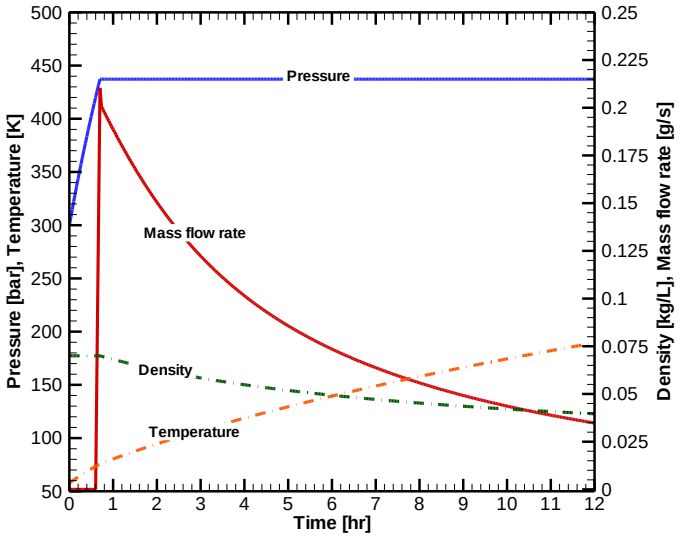

Figure 6. Pressure, mass flow rate, density and temperature of hydrogen as a function of time for the heating process with hydrogen extraction at MAWP (Strategy 2) for a vessel initially filled to 300 bar and 70 kg/m^3 (57.7 K) and hydrogen extraction at the minimum initial rate (2.10x10^{-4} kg H_2/s, 10.8 kW fuel cell power) to avoid exceeding the MAWP.

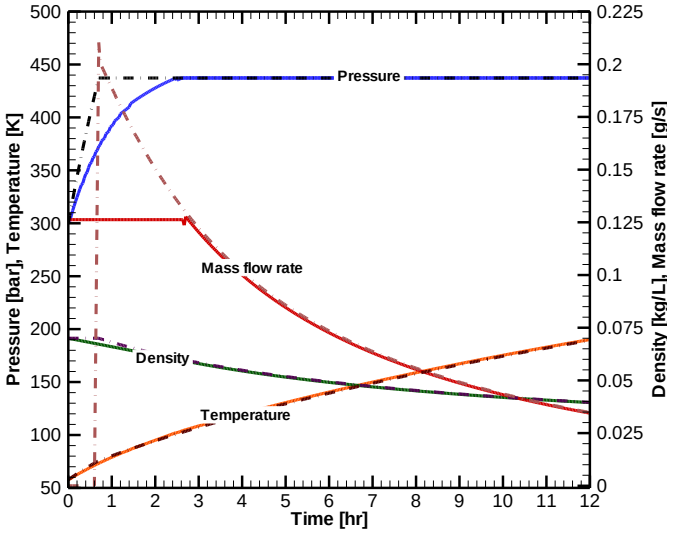

Figure 7. Pressure, temperature, mass flow rate and density for the two cases being considered: immediate H_2 extraction (Strategy 1, solid lines), and H_2 extraction at MAWP (Strategy 2, dotted lines). The information is repeated from Figures 5 and 7 for detailed comparison.

We finally consider the effect of H_2 storage density at the moment of vacuum insulation failure. This is important because vehicles are seldom parked after refueling to maximum density. Figs. 8 and 9 show maximum vessel pressure as a function of PEM fuel cell output power for several initial hydrogen storage densities (35-70 g/L) at 300 bar initial pressure. The figures show that the fuel cell output power necessary to avoid exceeding MAWP (437 bar, dotted line) decreases rapidly as the density is reduced, from 6.5 kW at 70 g/L to 0.5 kW at 35 g/L for Strategy 1 (Fig. 8), and from 10.8 kW at 70 g/L to 1 kW at 35 g/L for Strategy 2 (Fig. 9). The figures indicate that handling vacuum failure at H_2 densities below the maximum will typically be well within the capacity of the vehicle fuel cell and accessories.

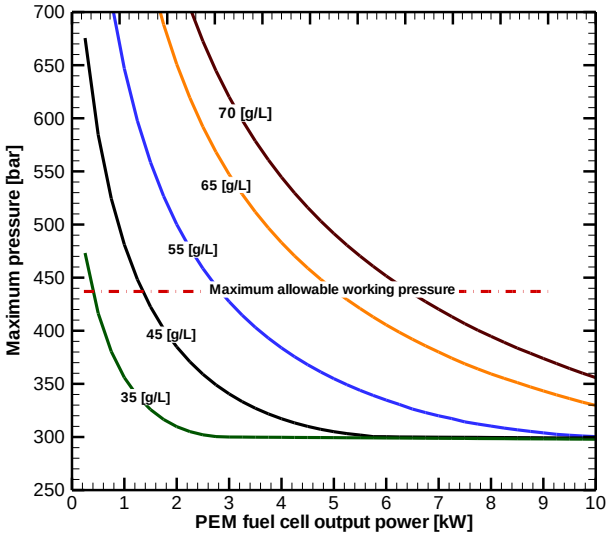

Figure 8. Maximum vessel pressure as a function of fuel cell output power for a vessel initially at 300 bar and 70, 65, 55, 45 and 35 g/L, considering that hydrogen extraction starts at the moment of vacuum insulation failure (Strategy 1).

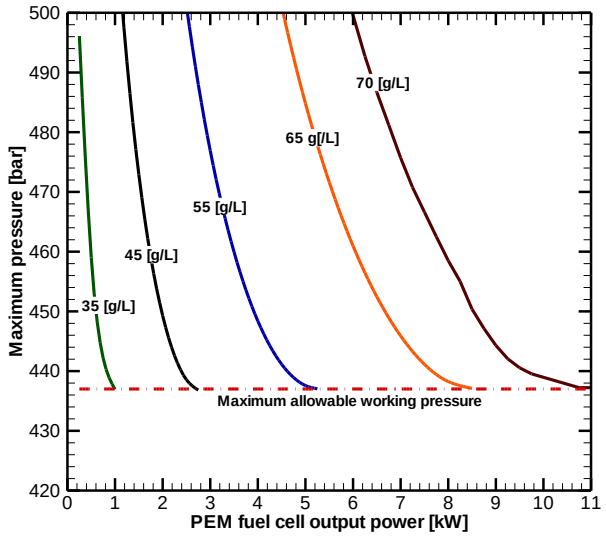

Figure 9. Maximum vessel pressure as a function of fuel cell output power for a vessel initially at 300 bar and 70, 65, 55, 45 and 35 g/L, considering that H_2 extraction starts when MAWP is reached (Strategy 2).

4. CONCLUSIONS

We have analyzed a critical subject for the safety of future vehicles powered by H_2 stored in cryogenic vessels: the possible consequences of vacuum insulation failure when the vehicle is in a closed space (e.g. in a garage or a tunnel). A failure in the vacuum insulation would cause a ~100X increase in heat transfer, resulting in rapid pressurization of the cryogenic vessel that, depending on the initial conditions (density and temperature) can force H_2 extraction to avoid exceeding the vessel MAWP.

Using a lumped thermodynamic model and taking into account non-ideal properties of hydrogen, we have calculated H_2 extraction rates from the cryogenic vessel, considering the most critical case in which the vessel is initially full at near maximum density (300 bar and 70 g/L). Instead of releasing H_2 to the environment, which could potentially lead to ignition, we consider the possibility of consuming the extracted H_2 in the fuel cell and dissipating the generated electricity onboard the vehicle, possibly operating the vehicle accessories (mainly the air conditioner) or charging the battery. Two strategies

were analyzed: in the first, H_2 extraction begins at the moment of vacuum system failure. In the second, H_2 extraction begins when the vessel reaches the maximum allowable working pressure (MAWP). The first strategy results in slower extraction rate, but requires sensors or computational strategies that can detect the failure of the vacuum system.

The results indicate that the thermodynamic advantage of cryogenic pressure vessels capable of containing H_2 and releasing it at a relatively high temperature results in low hydrogen extraction rates that can be consumed by a fuel cell (6.5 and 10.8 kW of electric power) without the need to release hydrogen to environment. Both strategies are thus feasible and the final decision depends on economic and/or implementation constraints.

ACKNOWLEDGMENTS

This work was sponsored by the Research and Graduate Studies Office (DAIP) of the University of Guanajuato and by Mexico's National Council of Science and Technology (CONACyT). This work performed under the auspices of the U.S. Department of Energy by Lawrence Livermore National Laboratory under Contract DE-AC52-07NA27344.

REFERENCES

1. Berry G.D, Martinez-Frias J., Espinosa-Loza F., Aceves S.M., Hydrogen Storage and Transportation, *Encyclopedia of Energy,* **3**, 2004, pp. 267-281.
2. Barthélémy H., Hydrogen Storage-Industrial Perspectives, *International Journal of Hydrogen Energy,* **37**, 22, 2012, pp. 17364-17372.
3. Jorgensen S. W., Hydrogen Storage Tanks for Vehicles: Recent Progress and Current Status, *Current Opinion in Solid State and Materials Science,* **15**, 2, 2011, pp. 39–43.
4. Durbin D. J., Malardier-Jugroot C., Review of Hydrogen Storage Techniques for on Board Vehicle Applications, *International Journal of Hydrogen Energy,* **38**, 34, 2013, pp. 14595-14617.
5. Aceves S. M., Espinosa-Loza F., Ledesma-Orozco E., Ross T. O., Weisberg A. H., Brunner T. C., Kircher O., High-Density Automotive Hydrogen Storage with Cryogenic Capable Pressure Vessels, *International Journal of Hydrogen Energy*, **35**, 3, 2010, pp. 1219–1226.
6. Aceves S. M., Petitpas G., Espinosa-Loza F., Matthews M. J., Ledesma-Orozco E., Safe, Long Range, Inexpensive and Rapidly Refuelable Hydrogen Vehicles with Cryogenic Pressure Vessels, *International Journal of Hydrogen Energy*, **38**, 5, 2013, pp. 2480-2489.
7. Aceves S. M., Berry G. D., Martinez-Frias J., Espinosa-Loza F., Vehicular Storage of Hydrogen in Insulated Pressure Vessels, *International Journal of Hydrogen Energy,* **31**, 15, 2006, pp. 2274 – 2283.
8. Aceves S. M., Berry G. D., Rambach G. D., Insulated Pressure Vessels for Hydrogen Storage on Vehicles, *International Journal of Hydrogen Energy*, **23**, 7, 1998, pp. 583-591.
9. Aceves S. M., Martinez-Frias J., Garcia-Villazana O., Analytical and Experimental Evaluation of Insulated Pressure Vessels for Cryogenic Hydrogen Storage, *International Journal of Hydrogen Energy,* **25**, 11, 2000, pp. 1075-1085.
10. Ahluwalia R. K., Hua T. Q., Peng J. K., On-Board and Off-Board Performance of Hydrogen Storage Options for Light-Duty Vehicles. *International Journal of Hydrogen Energy,* **37**, 3, 2012, pp. 2891-2910.
11. Petitpas G., Aceves S. M., The Isentropic Expansion Energy of Compressed and Cryogenic Hydrogen, *International Journal of Hydrogen Energy*, **39**, 35, 2014, pp. 20319-20323.
12. Petitpas G., Aceves S. M., Modeling of Sudden Hydrogen Expansion from Cryogenic Pressure Vessel Failure, *International Journal of Hydrogen Energy*, **38**, 19, 2013, pp. 8190-8198.
13. Kircher O., Greim G., Burtscher J., Brunner T., Validation of Cryo-Compressed Hydrogen Storage (CCH2) – a Probabilistic Approach, *in Proceeding of the International Conference on Hydrogen Safety*, San Francisco, 2011.

14. Markert F., Melideo D., Baraldi D., Numerical Analysis of Accidental Hydrogen Releases from High Pressure Storage at Low Temperatures, *International Journal of Hydrogen Energy*, **39**, 14, 2014, pp. 7356-7364.
15. Yan-Lei L. Jin-Yang, Z., Ping X., Yong-Zhi Z., Hai-Yan B., Hong-Gang C., Huston D., Numerical Simulation on the Diffusion of Hydrogen Due to High Pressured Storage Tanks Failure, *Journal of Loss Prevention in the Process Industries*, **22**, 3, 2009, pp. 265–270.
16. Cancelli C., Demichela M., Piccinini N., Accidental Release of Hydrogen from a Cryogenic Tank, *Cryogenics*, **45**, 7, 2005, pp. 481–488.
17. Ichard M., Hansen O. R., Middha P., Willoughby D., CFD Computations of Liquid Hydrogen Releases, *International Journal of Hydrogen Energy*, **37**, 22, 2012, pp. 17380-17389.
18. Prasad K., High-Pressure Release and Dispersion of Hydrogen in a Partially Enclosed Compartment: Effect of Natural and Forced Ventilation, *International Journal of Hydrogen Energy*, **39**, 12, 2014, pp. 6518-6532.
19. Aceves S. M., Berry G., Espinosa-Loza F., Petitpas G., Switzer V., Preliminary Testing of LLNL/Linde 875-bar Liquid Hydrogen Pump, *FY 2014 Annual Progress Report, DOE Hydrogen Program*, Washington, DC, 2014.
20. Bergman T. L., Lavine A. S., Incropera F. K., Dewitt D. P., Fundamentals of Heat and Mass Transfer, 2011, John Wiley & Sons, 7th. edition.
21. Leachman J., Fundamental Equations of State for Parahydrogen, Normal Hydrogen, and Orthohydrogen, *MS Thesis, University of Idaho*, 2007.
22. Lemmon E. W., Huber M. L., McLinden M. O., NIST's Standard Reference Database 23: Reference Fluid Thermodynamic and Transport Properties- REFPROP, *National Institute of Standards and Technology, Standard Reference Data Program*, Gaithersburg, 2007.
23. Barbir F., Gómez T., Efficiency and Economics of Proton Exchange Membrane (PEM) Fuel Cells, *International Journal of Hydrogen Energy*, **21**, 10, 1996, pp. 891-901.
24. Larminie J., Dicks A., Fuel Cell System Explained, 2003, Wiley, 2nd. edition.
25. Von Helmolt R., Eberle U., Fuel Cell Vehicles: Status 2007, *Journal of Power Sources*, **165**, 2, 2007, pp. 833–843.
26. Cho H., Park C., Experimental Investigation of Performance and Exergy Analysis of Automotive Air Conditioning Systems Using Refrigerant R1234yf at Various Compressor Speeds, *Applied Thermal Engineering*, **101**, 2016, pp. 30–37.